RESEARCH ARTICLE | NOVEMBER 03 2023

Development and assessment of a methodology for abstraction of topology optimization results to enable the substitution of optimized beams

Special Collection: Proceedings of the International Congress of Applications of Lasers & Electro-Optics (ICALEO 2023)

Tim Röver ; Maximilian Bader; Karim Asami ; Claus Emmelmann ; Ingomar Kelbassa

J. Laser Appl. 35, 042061 (2023)
https://doi.org/10.2351/7.0001185

Journal of Laser Applications ARTICLE pubs.aip.org/lia/jla

Development and assessment of a methodology for abstraction of topology optimization results to enable the substitution of optimized beams

Cite as: J. Laser Appl. 35, 042061 (2023); doi: 10.2351/7.0001185
Submitted: 17 July 2023 · Accepted: 5 October 2023 ·
Published Online: 3 November 2023

Tim Röver,[1,a)] Maximilian Bader,[1] Karim Asami,[1] Claus Emmelmann,[1] and Ingomar Kelbassa[2,3]

AFFILIATIONS

[1]Institute of Laser and System Technologies (iLAS), Hamburg University of Technology (TUHH), Harburger Schloßstraße 28, 21079 Hamburg, Germany
[2]Fraunhofer Research Institution for Additive Manufacturing Technologies IAPT, Am Schleusengraben 14, 21029 Hamburg, Germany
[3]Institute for Industrialization of Smart Materials (ISM), Hamburg University of Technology (TUHH), Eißendorfer Straße 40, 21073 Hamburg, Germany

Note: Paper published as part of the special topic on Proceedings of the International Congress of Applications of Lasers & Electro-Optics 2023.
[a)]**Electronic mail:** tim.roever@tuhh.de

ABSTRACT

Improving mechanical topology optimization (TO) results by substituting biomimetic beams is one possibility to achieve designs of mechanical components that are highly sustainable and show good mechanical performance. Because of their geometric complexity, such designs were found to be well-suited for production by laser additive manufacturing. One obstacle of incorporating biomimetics beams in TO designs is the lack of detailed design methodologies. Röver *et al.* ["Methodology for integrating biomimetic beams in abstracted topology optimization results," in *Proceedings of the ASME 2022 International Mechanical Engineering Congress and Exposition. Volume 4: Biomedical and Biotechnology; Design, Systems, and Complexity Columbus*, OH, 30 October–3 November (ASME, New York, 2022)] proposed a corresponding design concept. Building on their concept, we present in this work a detailed methodology for abstraction of TO results to a design consisting of ball nodes and cylindrical beams. Using such an auxiliary design, the internal forces and moments of the beams can be evaluated to allow for the substitution of suitable biomimetic beams to generate biomimetic component designs in a next step. We present a skeletonization algorithm based on the potential field approach. Using the skeletonization and an additional analysis of the dimensions of the beams in the TO result, the algorithm develops an auxiliary design of the original TO result. The final algorithm was applied to three common TO results to obtain one auxiliary component design each. The developed algorithm was found to generate abstractions that were well-suited for use in the methodology proposed in Röver *et al.* ["Methodology for integrating biomimetic beams in abstracted topology optimization results," in *Proceedings of the ASME 2022 International Mechanical Engineering Congress and Exposition. Volume 4: Biomedical and Biotechnology; Design, Systems, and Complexity Columbus*, OH, 30 October–3 November (ASME, New York, 2022)], because internal forces and moments in the abstracted beams could be evaluated with less effort. Therefore, our work contributes to a detailed design methodology for biomimetic mechanical components in the field of design for additive manufacturing.

Key words: design for additive manufacturing (DfAM), skeletonization, generative design, design optimization, biomimetics, topology optimization, finite element analysis, PBF-LB/M

INTRODUCTION

Lightweight structures are becoming increasingly relevant in the automotive and aerospace industries. A lower weight ensures that less energy is needed to move, i.e., less fuel is consumed. At the same time, the use of a lightweight structural element reduces the amount of manufacturing material that is consumed. It was suggested in previous work that by using bionic structures, the weight of structural designs developed by topology optimization (TO) can be further reduced while maintaining structural stability.[1]

Biomimetic structures are inspired by nature in order to transfer the modes of operation from biology to technical applications.[2] References 1 and 3 were one of the first works in which laser additive manufacturing and biomimetics were combined to generate novel designs for structural components. In both works, aviation applications were focused.

References 4 and 5 show the potential for performance and functionality increase of components and systems when combining additive manufacturing (AM) and biomimetics for a variety of applications. For a more comprehensive and general information on the field of biomimetics, the reader is kindly referred to Refs. 6–8.

Reference 9 proposed a concept for a detailed design methodology to generate biomimetic designs for structural components based on TO results. TO is a valuable tool in the design of components. However, considering material distribution–based TO approaches, the quality of the results depends on many factors, one of which is the resolution of the finite-element mesh.[10] Because of limited computational resources, the finite-element mesh cannot be refined infinitely, due to which the geometric complexity of the TO result is limited. The design methodology proposed in Ref. 9 aims to improve existing TO results by integrating biomimetic beams and redesigning nodes to achieve a higher geometric complexity of the design. The authors of the study assume that the increased geometric complexity allows for a lower mass of the component, while ensuring its structural integrity.

The methodology proposed in Ref. 9 generates designs that are producible by AM. It consists of the following steps:

- Input: The input is a result of a mechanical TO.
- Abstraction: The input abstraction algorithm develops an abstraction of the TO results in the form of a representation by points and lines using a potential field approach. In a next step, a 3D auxiliary abstraction of the input is developed. This 3D abstraction consists of cylindrical beams and ball nodes.
- Evaluation of internal forces and moments in beams: The internal forces and moments at cross sections at 20% and 80% of the length of the cylindrical beams of the auxiliary abstraction are evaluated.
- Database of biomimetic beams: For each of the cylindrical beams of the auxiliary abstraction, a biomimetic beam is developed. Development of the biomimetic beams is based on a database of beam designs and the information regarding internal forces and moments of the beams at the two analyzed cross sections and the beam's lengths.
- Generation of nodes: One of two approaches is used to develop a node for the new biomimetic component.
- Finite-element analyses of biomimetic component design: Biomimetic beams and the developed nodes are combined to achieve a complete component design. Finite-element analyses are used with possible returns to earlier steps of the methodology to ensure that the new design can support the expected loads.
- Output: The output is a design of a biomimetic component.

This work presents a detailed solution to the concept regarding abstraction proposed in Ref. 9. Moreover, it exemplarily shows how the outputs from the solution can be used for the evaluation of internal forces and moments in the beams of the abstraction.

MATERIALS

Implementation of the work was primarily done in COMSOL Multiphysics version 5.4.[11] Only the evaluation of internal forces and moments was done in COMSOL Multiphysics version 6.0.[12]

Structural steel was considered as the material of all mechanical structures in this work. Material parameters were obtained from the Comsol Multiphysics Material Library and are given in Table I.

ABSTRACTION METHODOLOGY

In the following section, the developed abstraction methodology is presented. First, the development of three different input TO results for the application of the abstraction methodology is presented. Next, the abstraction methodology itself is presented in detail. Figure 1 gives an overview over the respective steps. In the last subsection, the evaluation of internal forces and moments in the beam cross sections of one of the 3D abstractions is demonstrated. For more detailed information on the implementation of the abstraction methodology, the reader is kindly referred to the supplementary material,[13] which contains abstraction models of the Michell cantilever.

Input topology optimizations

In Figs. 2(a)–2(c), the design spaces, their dimensions, mechanical constraints, and the final TO results of three mechanical problem formulations are depicted. These TO results were developed as an input for the abstraction methodology of this work. In the following paragraphs, the generation of these results is briefly presented.

All three TO simulations are well known and often used as exemplary cases in the field of TO. The detailed problem design used in this work was based on Ref. 14. The three problems are referred to as Michell cantilever, L-shape, and Messerschmitt–Bölkow–Blohm (MBB) beam.

The Michell cantilever's design space has a length of 180 mm, a height of 60 mm, and a thickness of 10 mm. The cantilever is supported by a fixed clamping on one side. On the other side, a small surface is subjected to the mechanical load of 500 N in the

TABLE I. Material properties as considered in numerical analyses.

Property/alloy	Structural steel
Elastic modulus (GPa)	200
Poisson's ratio (−)	0.30
Density (kg/m^3)	7850

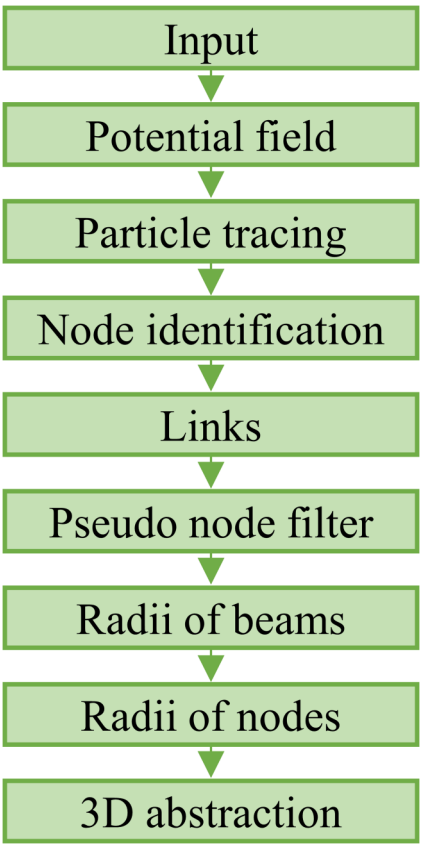

FIG. 1. Overview of the steps of abstraction methodology.

negative z-direction. The respective surface has a height of 6 mm and a width of 10 mm.

The L-shape's design space length of the long sides is 200 mm. The short sides have an edge length of 120 mm. A radius was added to the notch of the component in order to avoid stress peaks. The radius has a value of 20 mm. The model has a thickness of 10 mm. The component is mechanically fixed at the top surface. An area for load application was defined with a length of 20 mm. The load applied in the negative z-direction was defined as 600 N.

The MBB beam's design space has a length of 200 mm, a height of 40 mm, and a thickness of 10 mm. Mechanical boundary conditions for this model were partly based on Ref. 15. The bearings consist of a fixed clamping and a roller bearing. These are defined on the lower level of the model at each end. On the top side, an area of 10 mm length was created for load application. As before, the applied force is oriented in the negative z-direction and in this case has a value of 1000 N.

Hexahedral finite-element (FE) meshes were generated for all three TOs using the swept meshing function implemented in Comsol Multiphysics 5.4.[11] Maximum and minimum element sizes were chosen equally for the models and had values of 1 mm (Michell cantilever), 1.5 mm (L-shape), and 1 mm (MBB beam) based on Ref. 14.

The density-based solid isotropic material with penalization (SIMP) method, as implemented in Comsol Multiphysics 5.4[16] based on Refs. 17 and 18, was used to generate the TO results. In addition to the mechanical boundary conditions, an integral objective was implemented at all six outer surfaces of the TO models to hinder material to be distributed close to the outer areas of the design spaces. This simplifies the export of the TO results in the used software.

Relevant parameters of the TOs of this work are given by the penalty factor $p = 6$ and the volume fraction $v_f = 0.25$. The models were optimized in 70 optimization iterations.

Abstraction steps

The abstraction methodology was developed based on the concept proposed in Ref. 9, which itself was based on Refs. 19–22. Its output is a 3D component design that is an abstraction of the input TO result. The abstraction consists of cylindrical beams and ball nodes. The size of the cylindrical beams and ball nodes is based on the input TO result. It is noted that the abstraction is strongly connected to the research on curve skeletons. For a comprehensive overview of the topic, the reader is kindly referred to Ref. 23.

In the following subsections, the steps of the abstraction methodology are presented. An overview of the abstraction methodology is given by input, output, and selected interim results, as depicted in Fig. 3.

Input

Input for the developed abstraction methodology is given by TO results such as the ones depicted in Figs. 2(a)–2(c) and 3(a). They consist of 3D solids.

Potential field

A negative electric potential (V_0) is added to the surface of the TO design and a positive space charge density (ρ_v) is applied to the volume of the same. A static numerical simulation results in an electric field within the 3D volume with a minimal potential at the model surface and increasingly higher potentials toward the local cores. Therefore, the gradients are oriented from the "inside" to the "outside." An exemplary result of this step can be found in Fig. 3(b).

Particle tracing study

Building on the previous step, a certain number of particles (n_P) of negative charge are spread equally on the surface of the 3D volume. Figure 3(c) shows the particles (green) in their initial positions. These particles are subject to the electric field. Furthermore, a friction force with a background number density (N_d) is added to the study of moving particles. In a time-dependent numerical analysis, the particles then accumulate in various points within the 3D volume [cf. Fig. 3(e)]. The accumulation locations can be attributed to two groups. One group of particles accumulates close to the nodes of the TO design. The other group of particles grinds to a halt inside the beam-like structures that connect nodes. It is noted that the friction force ensures that the particles grind to a halt and prevent their oscillatory motion. The prevention of oscillation of

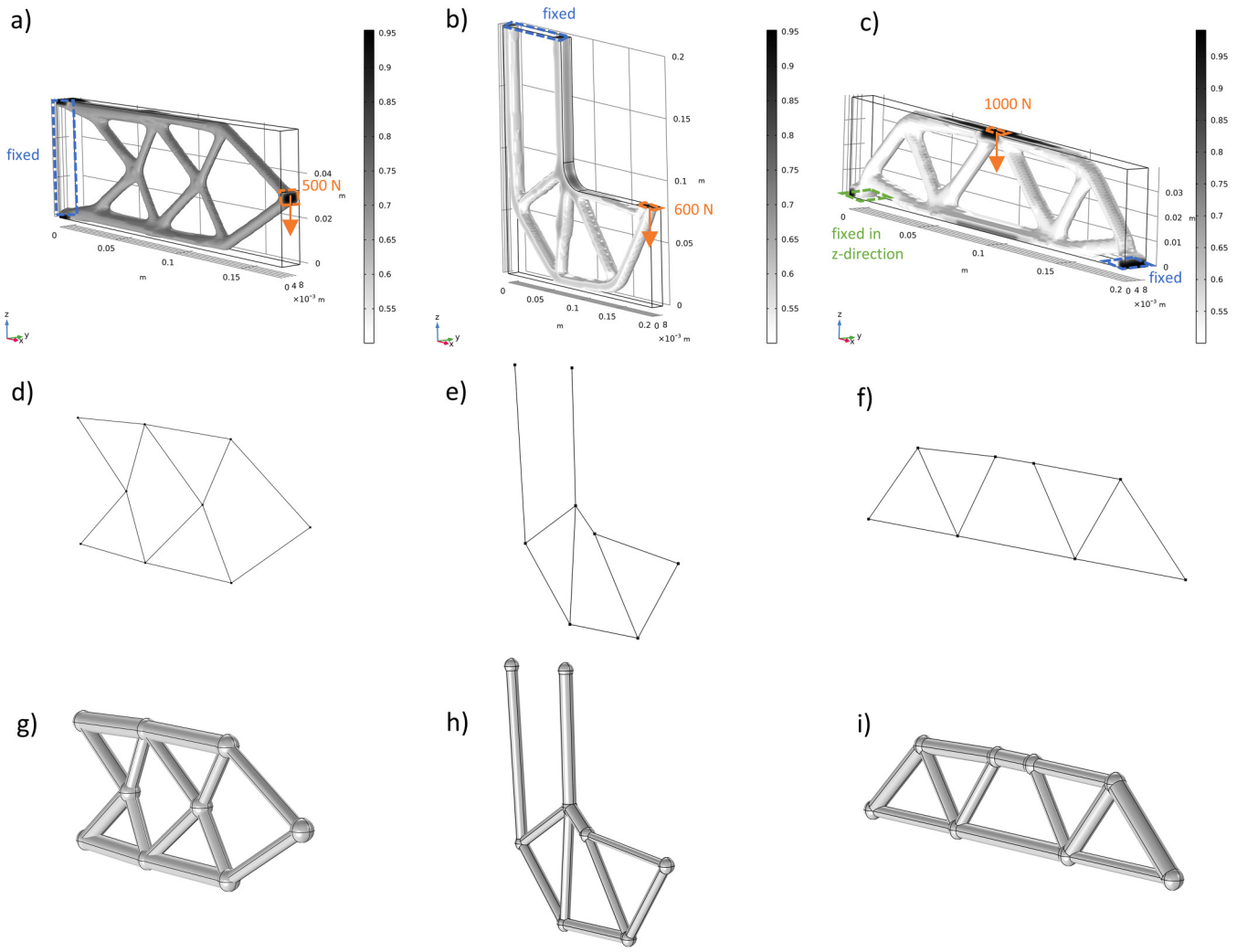

FIG. 2. (a)–(c) TO results developed as input for abstraction methodology. Relative densities are given by the scales. (d)–(f) Abstraction of TO results by lines and points, which are the interim results of the presented methodology. (g)–(i) 3D Abstractions of TO results by cylindrical beams and ball nodes.

particles is of high importance to ensure high-quality abstraction results.

Node identification

In a next step, accumulations of particles are identified. This is done by investigating the distances between the locations of the particles at the end of the time-dependent study. Starting with the first particle, all other particles that are within a defined small radius ($r_{\text{nodes\_filter}}$) are attributed to the same node. Moving on with the second particle, it is checked whether or not the particle was already attributed by the algorithm. If it was already attributed, the algorithm moves to the next particle. If it was not attributed, its final coordinates are defined as a new node and again all other particles that are within the $r_{\text{nodes\_filter}}$ are again attributed to this node. Therefore, a long list of the particles' final coordinates at the end of the time-dependent study is reduced to a list of nodes' coordinates.

Links

In a next step, connections between nodes are identified by analyzing the particles' initial locations at the beginning of the time-dependent study and their attribution to the nodes based on the previous step. A threshold $r_{\text{links\_filter}}$ is introduced. All possible initial particle locations of two particles are analyzed. If the distance between two initial locations of the two particles is within the threshold $r_{\text{links\_filter}}$ and both particles are attributed to two different nodes, a link is successfully identified. Figure 3(f) depicts an exemplary result after this step.

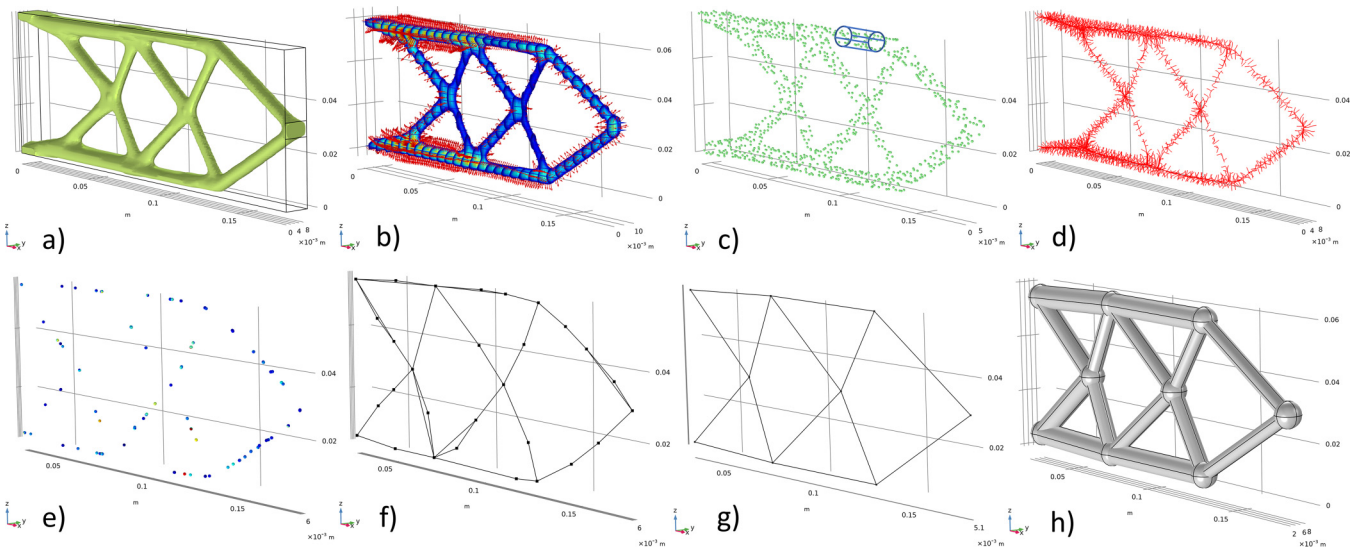

FIG. 3. Overview of the input, output, and interim results of the abstraction methodology.

Pseudo node filter

Next, a filter algorithm is applied to improve the interim abstraction result. One after another, all nodes of the interim results are analyzed that have one or two nodes connected to them by links. The angle between the two linking lines that connect the three nodes is analyzed. If the angle α is $153° < \alpha < 190°$, the center node is classified as a pseudo node. The pseudo node and its links are deleted and a direct link between the remaining two nodes is introduced. After all nodes are analyzed as previously explained, the same procedure is run once more for all remaining nodes to remove pseudo nodes that might have developed after the first filter cycle.

After filtering pseudo nodes using the presented method, an abstraction consisting of lines and points based on the true nodes and their links can be generated [cf. Fig. 3(g)].

Radii of beams

For generating 3D abstraction values, the radii of the cylindrical beams and ball nodes need to be defined. For each link connecting two nodes, the following is done: the linking line segment connecting the two nodes is reduced by 20% of its length at both ends. Then, a hypothetical cylinder is generated to be used as a probe. Figure 3(c) shows an exemplary cylindrical probe used for identifying the thickness of one of the beam-like structures in the TO result. The cylinder's axis is given by the previously reduced line segment. The radius of the cylinder $r_{\text{cyl\_probe}}$ is defined to be 10 mm for all three models in this work. A schematic of the cylindrical probe is depicted in Fig. 3(c). Considering the starting points of the particles at the beginning of the time-dependent study, all particles that are within the cylindrical probe are identified. These points are used to obtain a value for the thickness of the beam connecting the two nodes.

First, the regression line of all starting points within the probe is identified. For implementation, the Java package[24] was used. The position vector of the regression line is identified by using the average values for the x-, y,- and z-coordinates of all starting points, respectively.

The initial locations of the particles inside the cylindrical probe are then used to identify the direction vector of the regression line. For this, the x-, y,- and z-coordinates are saved into a matrix. From each entry, the corresponding value of the position vector is then subtracted. From this matrix, the covariance matrix is calculated by multiplying it with its respective inverse. The eigenvalues and eigenvectors of this covariance matrix are then determined by applying the power method based on Refs. 25 and 26. The eigenvector corresponding to the greatest eigenvalue is then set as the direction vector of the regression line.

For calculating the beam radius, the initial locations of the particles inside the cylindrical probe, the position vector, and the direction vector of the regression line are used. The distance between each initial particle location within the probe and the regression line is calculated. The distances of all particles are then averaged and this value is set as the radius of the beam of the abstraction.

Radii of nodes

The radii of all ball nodes in the abstraction are set to be 110% of the largest radius of any cylindrical abstraction beam as identified from the previous step.

3D Abstraction

Finally, an abstraction consisting of cylindrical beams and ball nodes can be generated. The abstraction is based on the input TO result. Figures 2(g)–2(i) and 3(h) show the respective abstractions for the three exemplary input TO results considered in this study.

Evaluation of internal forces and moments in abstractions

In Fig. 4, the results of evaluation of internal forces and moments in three exemplary beams of the abstracted TO result of the Michell cantilever are depicted. To achieve this result, the 3D abstraction consisting of cylindrical beams and ball nodes is subjected to the original mechanical boundary conditions of the Michell cantilever in a mechanical numerical analysis. Next, using the function of section forces as implemented in COMSOL Multiphysics 6.0,[27] the internal forces and moments at the three cross sections of the solid could be evaluated. For each cross section of a beam, the axial force (N), the shear force along the first local axis (T1), the shear force along the second local axis (T2), the twisting moment (Mt), the bending moment around the first local axis (M1), and the bending moment around the second local axis (M2) could be evaluated with low effort.

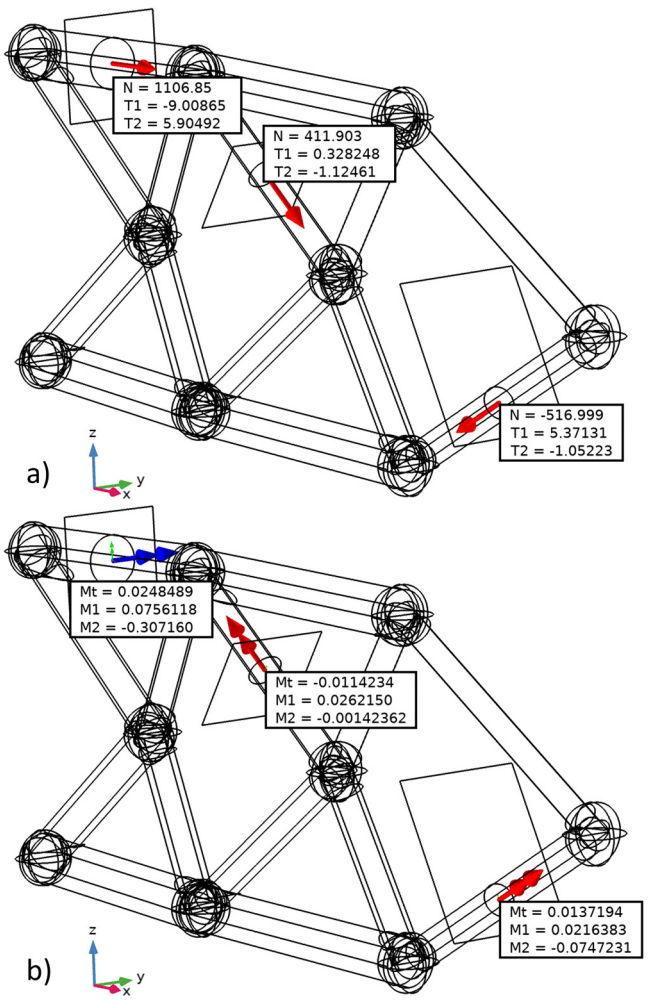

FIG. 4. Evaluation of internal forces and moments at three exemplary cut surfaces within beams of the abstracted TO result of the Michell cantilever. (a) Axial force (N), shear force along the first local axis (T1), and shear force along the second local axis (T2). (b) Twisting moment (Mt), bending moment around the first local axis (M1), and bending moment around the second local axis (M2).

Therefore, with regard to the methodology proposed in Ref. 9, it could be demonstrated that the evaluation of internal forces and moments in the beams of the 3D abstraction can be done with low effort.

The evaluation of internal forces and moments at 20% and 80% of the length of the beams, together with the information on the length of the beam that is known from the 3D abstraction, is expected to allow for the development and design of lightweight biomimetic beams according to Ref. 9 in a next step.

Hence, combining the abstraction methodology as proposed in this work with the functionality of sections forces, relevant parts of the methodology proposed in Ref. 9 were successfully developed and implemented.

DISCUSSION

In this section, the limitations and advantages of the presented work are presented and discussed.

Limitations

One limitation of the presented work is given by the choice of parameter values. Table II gives an overview over the most critical parameters of the abstraction methodology. Values for the parameters as used in this study were set based on preliminary studies on the three models. For application of the presented abstraction algorithm to other TO results, the authors expect that parameters need to be adjusted to achieve good abstraction results. A preliminary study on the impact of parameter choice on the abstraction results yielded that parameters $r_{\text{links\_filter}}$ and $r_{\text{nodes\_filter}}$ had a large impact on the quality of the abstraction result. This fact is one limitation of the work to be considered for future work on the topic.

Unbeneficial choice of parameters results in an abstraction as shown in Fig. 5. The algorithm did not filter all pseudo nodes.

TABLE II. List of the most relevant parameters of abstraction methodology.

Parameter	Explanation	Values used for Michell cantilever
$r_{\text{links\_filter}}$	Filter radius for identification of links between nodes	7 (mm)
$r_{\text{nodes\_filter}}$	Filter radius for identification of nodes	10 (mm)
$r_{\text{cyl\_probe}}$	Radius of cylindrical probe for evaluation of thickness of beams	10 (mm)
n_{P}	Number of particles	1000
V_0	Electric potential	−100 (V)
ρ_{v}	Space charge density	1×10^{-6} (C/m^3)
N_{d}	Background number density (of friction force)	5×10^{20} (1/m^3)
α	Upper and lower threshold angles of pseudo node filter	$153° < \alpha < 190°$

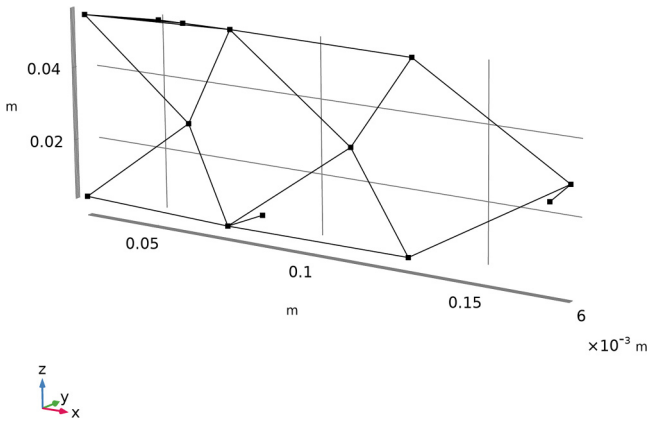

FIG. 5. Imperfect line and point abstraction of the Michell cantilever based on the use of alternative values for parameters ($r_{links\_filter} = r_{nodes\_filter} = 5$ mm).

Pseudo nodes that are linked to three other nodes are not filtered. Furthermore, pseudo nodes that have only one other node linked to them are not filtered either.

An additional limitation of the work is that the current abstraction methodology is not designed to develop abstractions for wall-like structures that might be part of the TO result. With regard to the methodology presented in Ref. 9, this is not problematic, as this methodology does not seem to focus on TO results with wall-like structures but rather seems to focus on truss-like TO results. However, if the abstraction methodology presented in this paper is to be used for another application or approach, the limitations with regard to wall-like structures should be considered.

Advantages

Implementation of the abstraction methodology in COMSOL Multiphysics has the advantage that the workflow from the setup of the TO to the evaluation of internal forces and moments in beams of the 3D abstraction can be done within one software. Further implementation of the overall methodology by Ref. 9 in COMSOL Multiphysics is expected to allow for the generation of a single executable file (EXE file) using the compiler function[28] to generate an user-friendly application that develops lightweight biomimetic component designs that are in line with design for additive manufacturing (DfAM).

This is expected to allow a widely automated design of structural components that are based on TO results as inputs. Such designs are expected to incorporate biomimetic beams to achieve a low mass, while ensuring structural integrity, and at the same time, consider the constraints by additive manufacturing techniques such as powder bed fusion of metals by a laser beam (PBF-LB/M).

SUMMARY AND OUTLOOK

A methodology for the abstraction of 3D TO results was presented. The methodology is based on previous works in the field of curve skeletons and was implemented in COMSOL Multiphysics.

Using an input TO result, a time-dependent particle tracing study is used to identify point nodes and line links for the abstraction based on the potential field approach. Filtering of the result is done for improvement of the interim result. Next, a submethodology for defining suitable dimensions of the cylindrical beams and ball nodes is applied to allow for generation of the final 3D abstraction of the input TO result.

The developed methodology was applied to three common mechanical problem formulations, and it was able to provide suitable 3D abstractions as outputs.

After applying the original mechanical loads to the 3D abstractions, the internal forces and moments at the cross sections in the beams can be evaluated with low effort. Therefore, the presented work gives detailed solutions to the first two steps of the more comprehensive design methodology for the biomimetic mechanical components proposed in Ref. 9 and contributes to the field of DfAM.

The authors plan to improve the presented work in the future by developing solutions for providing an automated choice of the relevant abstraction parameters. Furthermore, future work should focus on substitution of solid beams by biomimetic lightweight design beams and assess the generated biomimetic design with regard to lightweight characteristics and manufacturability in PBF-LB/M.

ACKNOWLEDGMENTS

Parts of this work were funded by the Fraunhofer Future AM project.

AUTHOR DECLARATIONS

Conflict of Interest

The authors have no conflicts to disclose.

Author Contributions

Tim Röver: Conceptualization (lead); Investigation (equal); Methodology (lead); Supervision (lead); Validation (equal); Visualization (lead); Writing – original draft (lead); Writing – review & editing (equal). **Maximilian Bader:** Conceptualization (supporting); Investigation (equal); Methodology (supporting); Validation (equal); Visualization (equal); Writing – original draft (equal); Writing – review & editing (supporting). **Karim Asami:** Conceptualization (supporting); Methodology (equal); Writing – original draft (supporting); Writing – review & editing (supporting). **Claus Emmelmann:** Conceptualization (supporting); Methodology (equal); Writing – review & editing (supporting). **Ingomar Kelbassa:** Writing – original draft (supporting); Writing – review & editing (equal).

REFERENCES

[1]C. Emmelmann, M. Petersen, J. Kranz, and E. Wycisk, "Bionic Lightweight Design by Laser Additive Manufacturing (LAM) for aircraft industry," Proc. SPIE **8065**, 80650L (2011).
[2]N. F. Lepora, P. Verschure, and T. J. Prescott, "The state of the art in biomimetics," Bioinspir. Biomim. **8**, 013001 (2013).

[3]C. Emmelmann, P. Sander, J. Kranz, and E. Wycisk, "Laser additive manufacturing and bionics: Redefining lightweight design," Phys. Procedia **12**, 364–368 (2011).
[4]M. Gralow, F. Weigand, D. Herzog, T. Wischeropp, and C. Emmelmann, "Biomimetic design and laser additive manufacturing—A perfect symbiosis?," J. Laser Appl. **32**, 21201 (2020).
[5]A. Du Plessis, C. Broeckhoven, I. Yadroitsava, I. Yadroitsev, C. H. Hands, R. Kunju, and D. Bhate, "Beautiful and functional: A review of biomimetic design in additive manufacturing," Addit. Manuf. **27**, 408–427 (2019).
[6]W. Nachtigall, *Bionics by Examples: 250 Scenarios from Classical to Modern Times*, 2015th ed. (Springer International, Cham, 2015).
[7]M. H. Dickinson, "Bionics: Biological insight into mechanical design," Proc. Natl. Acad. Sci. U.S.A. **96**, 14208–14209 (1999).
[8]B. Bhushan, "Biomimetics: Lessons from nature—An overview," Philos. Trans. Math. Phys. Eng. Sci. **367**, 1445–1486 (2009).
[9]T. Röver *et al.*, "Methodology for integrating biomimetic beams in abstracted topology optimization results," in *Proceedings of the ASME 2022 International Mechanical Engineering Congress and Exposition. Volume 4: Biomedical and Biotechnology; Design, Systems, and Complexity, Columbus, Ohio, 30 October–3 November* (ASME, New York, 2022).
[10]M. P. Bendsøe, M. P. Bendsøe, and O. Sigmund, *Topology Optimization: Theory, Methods and Applications* (Springer, Berlin, 2003) [Online], see http://www.loc.gov/catdir/enhancements/fy0815/2002030512-d.html
[11]COMSOL, see https://doc.comsol.com/5.4/doc/com.comsol.help.comsol/COMSOL_ReferenceManual.pdf for "Reference Manual: Version: Comsol Multiphysics 5.4 [Online]" (accessed May 25 2023).
[12]COMSOL, see https://doc.comsol.com/6.0/doc/com.comsol.help.comsol/COMSOL_ReferenceManual.pdf for "Reference Manual: Version: Comsol Multiphysics 6.0 [Online]" (accessed Mar. 31 2023).
[13]T. Röver, M. Bader, K. Asami, C. Emmelmann, and I. Kelbassa, see https://doi.org/10.15480/882.8168 for "Supplementary material to article with title: Development and assessment of a methodology for abstraction of topology optimization results to enable the substitution of optimized beams" (2023) [Online].
[14]G. Fiuk and M. W. Mrzygłód, "Numerical benchmarks for topology optimization of structures with stress constraints," Bull. Pol. Acad. Sci. Tech. Sci. **69**, e139317 (2021) [Online], see http://journals.pan.pl/Content/121172/PDF/Z_18_02049_Bpast.No.69(6)_OK.pdf
[15]O. Sigmund, "A 99 line topology optimization code written in matlab," Struct. Multidiscip. Optim. **21**, 120–127 (2001).
[16]COMSOL, see https://doc.comsol.com/5.4/doc/com.comsol.help.opt/OptimizationModuleUsersGuide.pdf for "Optimization module user's guide: Version: Comsol Multiphysics 5.4 [Online]" (accessed May 25 2023).
[17]M. P. Bendsøe, "Optimal shape design as a material distribution problem," Struct. Optim. **1**, 193–202 (1989).
[18]M. P. Bendsøe and N. Kikuchi, "Generating optimal topologies in structural design using a homogenization method," Comput. Methods Appl. Mech. Eng. **71**, 197–224 (1988).
[19]A. Nana, J.-C. Cuillière, and V. Francois, "Automatic reconstruction of beam structures from 3D topology optimization results," Comput. Struct. **189**, 62–82 (2017).
[20]J.-C. Cuillière, V. François, and A. Nana, "Automatic construction of structural CAD models from 3D topology optimization," Comput. Aided Des. Appl. **15**, 107–121 (2018).
[21]N. Ahuja and J.-H. Chuang, "Shape representation using a generalized potential field model," IEEE Trans. Pattern Anal. Mach. Intell. **19**, 169–176 (1997).
[22]N. D. Cornea, D. Silver, X. Yuan, and R. Balasubramanian, "Computing hierarchical curve-skeletons of 3D objects," Vis. Comput. **21**, 945–955 (2005).
[23]N. D. Cornea, D. Silver, and P. Min, "Curve-skeleton properties, applications, and algorithms," IEEE Trans. Vis. Comput. Graph. **13**, 530–548 (2007).
[24]J. Hicklin *et al.*, see https://math.nist.gov/javanumerics/jama/ for "JAMA: A Java Matrix Package: The MathWorks and the National Institute of Standards and Technology (NIST) (2012) [Online]" (accessed July 11 2023).
[25]M. Hermann, *Numerische Mathematik*, 2nd ed. (Oldenbourg Verlag, Munich, 2006).
[26]R. V. Mises and H. Pollaczek-Geiringer, "Praktische verfahren der gleichungsauflösung," Z. Angew. Mathematik Mechanik. **9**, 58–77 (1929).
[27]COMSOL, see https://doc.comsol.com/6.0/doc/com.comsol.help.sme/StructuralMechanicsModuleUsersGuide.pdf for "Structural mechanics module user's guide: Version: Comsol Multiphysics 6.0 [Online]" (accessed July 11 2023).
[28]COMSOL, see https://doc.comsol.com/6.0/doc/com.comsol.help.comsol/COMSOL_ApplicationBuilderManual.pdf for "Application builder reference manual: Version: Comsol Multiphysics 6.0 [Online]" (accessed July 11 2023).